Adsorption isotherm

The adsorption characteristics of EY dye onto wood saw dust was consistent with the Langmuir adsorption model which can be written according to equation 2 [17].

$$\frac{C_e}{q_e} = \frac{1}{q_m b} + \frac{C_e}{q_m} \qquad (2)$$

where C_e is the equilibrium concentration of adsorbate (mg/l), q_e is the amount of adsorbate adsorbed per unit mass of the adsorbent (mg/g), b is the Langmuir adsorption constant which is related to affinity between the adsorbate and the adsorbent while q_m is the theoretical monolayer saturation capacity. From the Langmuir equation, a plot of $\frac{C_e}{q_e}$ versus C_e should be linear if the Langmuir assumptions are valid. **Figure 2** presents the Langmuir isotherm for the adsorption of EY dye from aqueous solution onto wood saw dust. Langmuir adsorption parameters calculated from the slope and intercept of the plot were q_m = 14.29 mg/g and b = 0.044. The calculated q_m value is comparable to those reported for other dyes. For example, [20] reported q_m value of 12.83 mg/g for the adsorption of crystal violet dye onto Moroccan pyrophyllite, Banerje and Chattopadhyaya [21] obtained q_m value of 3.39 mg/g for terazine dye adsorbed on activated carbon, obtained q_m values of 8.947 mg/g for methyl green adsorbed on regia resin.
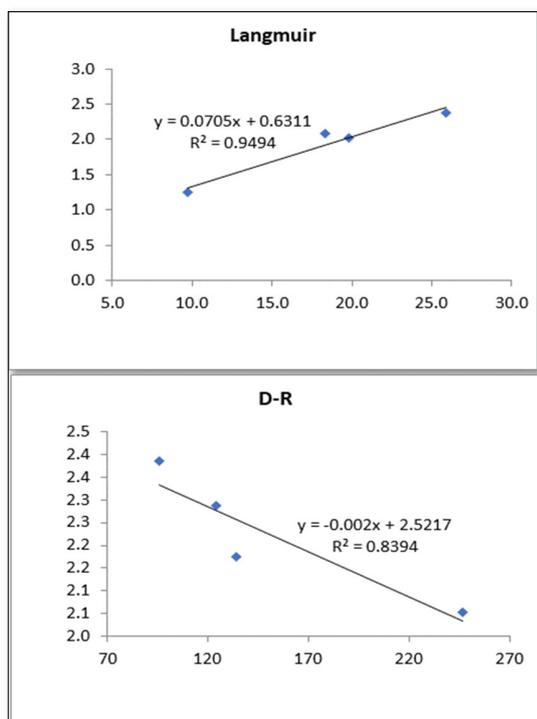

Figure 2. Langmuir and Dubinin-Radischkevich (DR) isotherms for the adsorption of EY dye unto wood saw dust respectively.

The Langmuir separation factor (R_L) define din equation 3, is a useful index for differentiating between favorable or unfavourable adsorption [22].

$$R_L = \frac{1}{(1+q_m C_0)} \qquad (3)$$

Consequently. if R_L values lie between 0 and 1, the adsorption is favourable. When R_L = 0 the adsorption is irreversible, when R_L value is equal to unity, a linear adsorption is favoured and R_L greater than unity indicates unfavorable adsorption [23]. Calculated R_L values were 0.003088, 0.002561, 0.005933, 0.005933 and 0.005922 for EY dye concentrations of 41 to 51 mg/L respectively. Therefore, the adsorption of EY dye onto wood sawdust is favorable at all concentrations.

The Dubinin-Radushkevich isotherm [24] is significant in describing the adsorption mechanism of an adsorbate unto homogenous and heterogeneous surfaces. The model is expressed according to equation 8.

$$q_e = q_m e^{-\beta \varepsilon^2} \qquad (8)$$

Mathematical form of applying the above equation is to convert it to a linear model using logarithm function as shown below,

$$q_e = lnq_m - \beta \boldsymbol{\varepsilon^2} \qquad (9)$$

where q_m is the Dubinin-Radushkevich (D-R) monolayer capacity (mmol/g), and ε is the polanyl potential defined according to equation 20 while β is a constant that is related to the adsorption energy, E (equation 11)

$$\varepsilon = RTln\left(1 + \frac{1}{C_e}\right) \qquad (10)$$

$$E = \frac{1}{\sqrt{2\beta}} \qquad (11)$$

Adsorption energy less than 8 kJ/mol point toward physical adsorption mechanism while adsorption energy in the range of 8 to 16 kJ.mol indicates that the adsorption is govern by exchange mechanism. However, adsorption energy greater than 16 kJ/mol is consistent with the prevalence or domination of particle diffusion [25]. Calculated value of the adsorption energy (22.36 J/mol) for EY dye indicates that chemisorption mechanism is partly involved in the adsorption of EY dye and also confirms the existent of particle diffusion.

The Gibb Helmholtz equation can be written as follows [26].

$$\Delta G^* = -2.303 RT log k_C \qquad (12)$$

Evaluated values of standard free energy changes from both Langmuir (-13.67 kJ/mol) and Temkin (-16.97 kJ/mol) isotherm constants were comparable and led to the conclusion that the adsorption of EY dye onto wood saw

dust is spontaneous and support the mechanism of physiosorption.

In adsorption study, the equilibrium amounts adsorbed (q_e) andequilibrium concentration (C_e) are related to the equilibrium constant according to the following equation,

$$k_c = \frac{q_e}{C_e} \qquad (13)$$

Also, from thermodynamics,

$$\Delta G^* = \Delta H^* - T\Delta S^* \qquad (14)$$

Therefore,

$$-2.303RT\log k_p = \Delta H^* - T\Delta S^* \qquad (15)$$

$$-T\ln k_p = \Delta H^* - T\Delta S^* \qquad (16)$$

$$\ln k_p = \frac{\Delta S^*}{R} - \frac{\Delta H^*}{RT} \qquad (17)$$

Therefore, a plot of $\ln k_p \, versus \, \frac{1}{T}$ is expected to be linear with slope and intercept equal to $\frac{\Delta H^*}{R}$ and $\frac{\Delta S^*}{R}$ respectively.

The plot obtained (plot not shown) indicated R^2 value of 0.965 while slope and intercept were -0.007 and -0.055 respectively. . Estimated values of ΔH^* and ΔS^* were -0.0582 J and -0.4572 J indicating that the adsorption of EY dye onto the surface of wood saw dust is exothermic and occurs in the direction of increasing degree of orderliness.

Kinetic Study

Pseudo first order and pseudo second order kinetics models can be expressed according to equations 18 and 19 respectively [27].

$$\ln(q_e - q_t) = \ln q_e - k_1 t \qquad (18)$$

$$\frac{t}{q_t} = \frac{1}{k_2 q_e^2} + \frac{t}{q_e} \qquad (19)$$

Agreement of the present adsorption data with pseudo first and second order kinetics was established through linear plots of $\ln(q_e - q_t)$ versus t and $\frac{t}{q_t}$ versus t for pseudo first and second order kinetics respectively (as shown in **Figure 3**). Calculated adsorption kinetic data (**Table 1**) are k_1= 0.096/m and k_2= 2.3 x 10^5 /m respectively while $\ln q_e$ (pseudo first order plot) and q_e (pseudo second order plots) were 0.009 and 6666.67 respectively. Perfect degree of fitness was obtained for the pseudo first order kinetics (R^2 = 1.000) compared to R^2 = 0.9462 obtained for pseudo second order kinetics. Consequently, adsorption of EY dye onto wood saw dust best fitted the pseudo first order kinetics than pseudo second order kinetics. Also, from the pseudo second order kinetic data, the initial adsorption rate (i.e. h) and half adsorption time ($t_{0.5}$) were calculated using the formula,

$$h = \frac{1}{k_2 q_e^2} \text{ and } t_{0.5} = \frac{1}{k_2 q_e} \text{ respectively [28].}$$
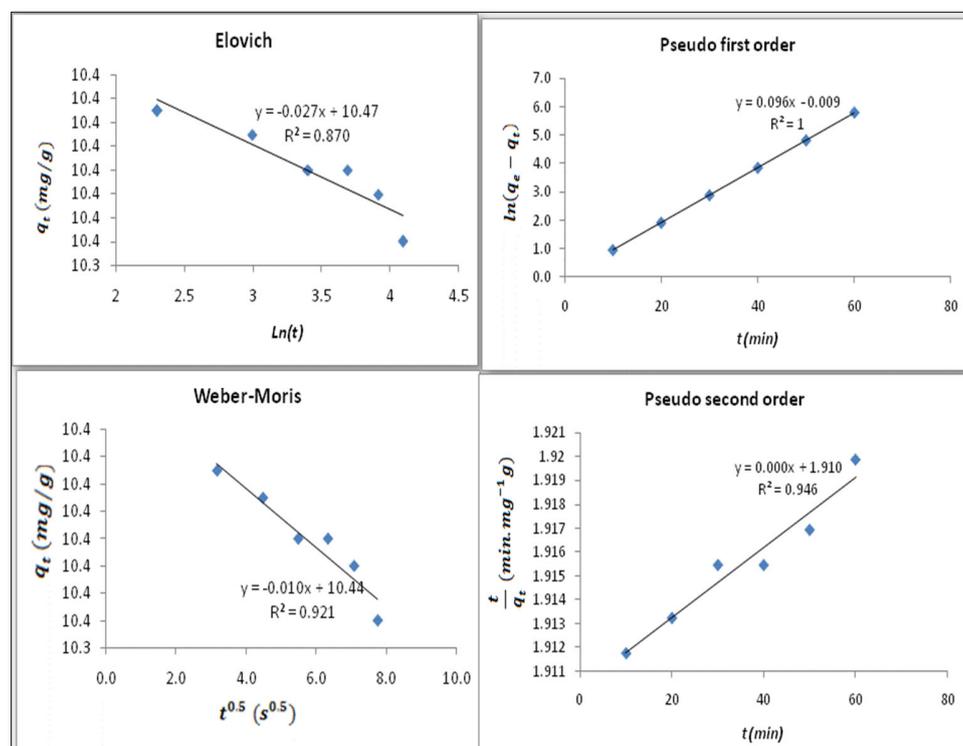

Figure 3. Elovich, Weber-Moris, pseudo first order and pseudo second order kinetic plots for the adsorption of EY dye on wood sawdust.

The Elovich equation is a kinetic model that is most suitable for explaining chemisorptions and for adsorption process that does not approach equilibrium at ease due to low surface coverage. Expression for the Elovich equation [29] can be written as:

$$q_t = \frac{1}{\beta}\ln(\alpha\beta) + \frac{1}{k_{Des}}lnt \qquad (20)$$

where α is the initial adsorption rate in mg/g/min, k_{Des} is desorption constant and is related to the activation energy of a chemisorption process and the extent of surface coverage. The adsorption of EY dye on the surface of wood saw dust fitted the Elovich adsorption model ($R^2 = 0.870$) as shown in a linear plot **(Figure 3)** of q_t versus t. Therefore, the mechanism of adsorption of EY dye partly involves chemisorptions. Estimated β value was 370. 37 whilesα was 58.95 mg/g/min.The Weber-Morris adsorption model (expressed as equation 21) is the most useful kinetic model for investigating intra particle diffusion [30].

$$q_t = B + K_{id}\sqrt{t} \qquad (21)$$

Kid is the intra particle diffusion constant (mg (g. min0.5) while B is the initial adsorption (mg/g). When B is zero,

intra particle diffusion is the rate controlling step. The Weber-Morris plot for the adsorption of EY dye (Figure 3) indicated a non-zerointercept (i.e. B = 10.44 mg/g) which implies that other mechanism also contributes to the adsorption of EY dye on wood sawdust (in addition to intra particle diffusion). Estimated kid value was 0.010 (mg (g. min0.5).

FTIR study

FTIR spectra of EY dye and that of the wood saw dust before and after adsorption were analyzed (spectra not shown). Frequencies and intensities of IR adsorption deduced from the FTIR of wood saw dust before and after adsorption of EY dye (spectra not shown) are presented in **Table 1**. The FTIR spectrum of EY dye indicated the presence of OH stretch at 3335 cm-1 (42.76 %), C0H stretch at 2117 (95.72 %), C=C stretch at 1640 (64.87 %) and C-N stretch at 1242 (88.535 %).

From **Table 1**, it can be deduced that the wood saw dust possess several functional groups that aided the adsorption of EY dye.

Table 1. Wave number and intensity of IR absorption by wood saw dust before and after adsorption of EY dye.

Wood saw dust		Wood saw dust after adsorption		Assignment
Wave number (cm⁻¹)	Intensity	Wave number (cm⁻¹)	Intensity	
3320	80.64	3339	91.10	OH stretch
2988	93.47	2895	94.03	C-H stretch
		2218	97.31	C≡Catretch
2106	96.13	2117	97.10	C=C stretch
		2009	97.61	C=C=N stretch
1990	97.40			C=C=C stretch
1961	96.71			C=C=C stretch
1905	96.73			C=C=C stretch
1737	93.71	1737	94.40	C=O stretch
1655	93.18	1640	93.41	C=O stretch
1596	91.89	1596	92.07	C=N stretch
1503	92.92	1503	93.19	C=O stretch
1482	91.35	1482	92.59	C=C stretch
1424	90.47	1424	90.70	OH bending
1369	90.65	1369	91.26	S=O stretch
1324	89.95	1324	90.28	S=O stretch
1286	87.80			C-O stretch
		1235	88.56	C-O stretch
1160	87.68	1160	88.41	C-O stretch
1108	81.75	1108	82.22	C-O stretch
1033	71.09	1033	72.96	C-OH stretch
		899	88.23	C-H bend
836	88.99	836	89.94	C-Cl stretch
672	81.72			C-Br stretch

After adsorption of ET dye, some functional groups were missing in the spectrum including C-Br stretch, C-O stretch at 1286 cm^{-1} and C=C=C stretches at 1990, 1961 and 1905 cm^{-1} respectively. The missing functional groups might have been used for the formation of new bonds [31]. However, new functional groups formed were C≡C stretch at 2218 cm^{-1}, C=C=N stretch at 2009 cm^{-1} and C-H bend at 899 cm^{-1}. The OH stretch at 3320 was shifted to 3339 cm^{-1} after adsorption of EY dye other included C-H stretch at 2988 shifted to 2895 cm^{-1}, C=C stretch at 2106 shifted to 2117cm^{-1} and the C=O stretch shifted from 1655 to 1640 cm^{-1}, The shift in frequencies of adsorption indicate that there is interaction between the adsorbent and the adsorbate [15, 16]. Functional groups that witness shift in intensity of adsorption (but not frequency) were C-Cl stretch at 836 cm^{-1}, C-OH stretch at 1033 cm^{-1}, C-O stretches at 1108 and 1160 cm^{-1} respectively, S=O stretches at 1324 and 1369 cm^{-1} respectively, OH bend at 1424 cm^{-1}, C=C stretch at 1482 cm^{-1}, C=O stretch at 1503 cm^{-1} C=N stretch at 1596 cm^{-1} and C=O stretch at 1737 cm^{-1}. Bathochromic and hypsochromic shifts in intensity confirms that the absorption strength of the adsorbent has been altered by the interaction between the dye and the adsorbent [17].

COMPUTATIONAL CHEMISTRY STUDY

Semiempirical parameters

Semiempirical parameters calculated for EY dye were E_{HOMO} (-7.787021 eV), E_{LUMO} (-1.107504 eV), total energy (-193.1411 eV), binding energy (-4197.2663 eV), isolated atomic energy (-117000.6061 eV), electronic energy (-902517.1837 eV), core interaction (781319.3113 eV) and heat of formation (-10.3993 kCal). The calculated semiempirical parameters are not at variance with those reported for good adsorbent for other dyes. For example [11] reported -8.4071 and -1.6856 eV as values of E_{HOMO} and E_{LUMO} for methylene blue and malachite green respectively (that were excellently adsorbed on neem leaves). However, their calculated electronic energies were -528,742.2598 and -885,289.2176 eV respectively (which is significantly less than that of EY dye). Other parameters were also relatively comparable [11] In EY dye, 29%, 25%, 22% and 23% of the HOMO electron population resides in the S, P_x, P_y and P_z orbitals. Adsorption is a surface phenomenon that involves charge or electron transfer or sharing. According to the frontier molecular orbital theory, the formation of adsorption bond (i.e. van der Waal for physical adsorption or chemical bond for chemisorption mechanism) involves interaction between the HOMO and LUMO molecular orbitals and the extent and readiness of the transfer depends on the energy gap [32] E_{HOMO} is an index that reflects tendency toward adsorption while E_{LUMO} indicates tendency toward desorption [33,34] Calculated energy gap is relatively low and suggest ease of adsorption governed by the proposed physical adsorption [34] **Fukui function.**

A neutral atom having N number of atoms can align in two different ways, either by losing or gaining electron. Such attacks lead to either nucleophilic or electrophilic attack respectively. Losing of one electron leaves the system as N-1 while gaining of one electron changes it to a N-1system. Apart from variation of electron, there is also variation of charge since donation or acceptance of electron also affects the charge of the molecule. Adsorption occurs via the transfer of charge from charged adsorbate to charge adsorbent surface (physical adsorption) or through the transfer of electron from the adsorbate to the adsorbent and vice versa (chemical adsorption). The Fukui function originates from the concept of considering the reactivity of a molecule in terms of the individual atom as it gains or loses electron. The finite difference approximation defines the three different types of Fukui function [33-35] as follows:

$$f_x^+ = q_{N+1} - q_N \qquad (22)$$

$$f_x^- = q_N - q_{N-1} \qquad (23)$$

$$f_x^0 = \frac{[(q_{N+1}) - (q_{N-1})]}{2} \qquad (24)$$

In analyzing the results obtained from Fukui function calculations, it is necessary to consider the most favorable behavior that will favor each atom on the molecule. The difference between nucleophile and electrophilic Fukui functions (equation 25) is an index that allows the prediction of the location where nucleophilic or electrophilic Fukui function resides [32,36-39]:

$$\Delta f_x = f_x^+ - f_x^- \qquad (25)$$

Consequently, if $\Delta f_x > 0$, the site is favourable to nucleophilic attack but if $\Delta f_x < 0$, the site is favourable to electrophilic attack. Calculated values of f_x^+, f_x^-, f_x^0 and Δf_x for both Ab initio and DFT levels are recorded in **Table 2**. The results expose various sites with positive values of Δf_x for both Ab initio and DFT calculations. However, highest values of f_x^+ for ab initio (0.0132) and DFT (0.0099) were obtained for O (26) which indicate that nucleophilic attack is likely located in this site [32, 40-43]. The Mayer bond order for this bond is also less than unity. Similarly, both ab initio and DFT predictions for the site for electrophilic attack did not prefer any other side but C(15) which has the highest positive values of f_x^- and highest negative value of Δf_x for both ab initio and DFT levels of theory. All the valence electron in C (15) are bonded suggesting that the attack will certainly involves a bond or functional group associated with C (15). Also, the total nuclear charge for O (26), Muliken atomic charge, Mayer total valence and Mayer bonded valence (Table 2) are 8.0, -0.617, 1.9961 and 1.9961 respectively. This also suggests that nucleophilic attack will preferably involves a bond or functional group and not the atom alone [44-46].

Table 2. Ab initio Fukui function for adsorption of EY dye.

Atom/No	Ab Initio			DFT		
	f_x^+	f_x^-	$f_x^+ - f_x^-$	f_x^+	f_x^-	$f_x^+ - f_x^-$
1 C	-0.0009	-0.0073	0.0064	-0.0013	-0.0046	0.0033
2 C	-0.0005	-0.0111	0.0106	-0.0054	-0.0248	0.0194
2 C	0.0027	-0.0116	0.0143	0.0033	-0.0058	0.0091
4 C	-0.0031	-0.0150	0.0119	-0.0064	-0.0426	0.0362
5 C	0.0034	-0.0102	0.0136	0.0038	0.0016	0.0022
6 C	-0.0019	-0.0232	0.0213	-0.0037	-0.0511	0.0474
7 C	0.0015	-0.0078	0.0093	0.0023	-0.0194	0.0217
8 C	0.0008	-0.0204	0.0212	-0.0024	-0.0530	0.0506
9 C	-0.0047	-0.0114	0.0067	-0.0014	-0.0067	0.0053
10 O	0.0007	-0.0144	0.0151	0.0010	-0.0176	0.0186
11C	-0.0022	-0.0128	0.0106	-0.0044	-0.0049	0.0005
12 C	0.0033	-0.0097	0.013	0.0026	-0.0284	0.031
13 C	-0.0011	-0.0027	0.0016	0.0013	-0.0117	0.013
14 C	0.0046	-0.0151	0.0197	0.0021	-0.0205	0.0226
15 C	-0.0009	0.0066	-0.0075	-0.0010	0.0213	-0.0223
16 C	-0.0003	0.0043	-0.0046	-0.0018	0.0029	-0.0047
17 C	-0.0035	-0.0068	0.0033	-0.0098	-0.0154	0.0056
18 C	-0.0033	-0.0066	0.0033	-0.0077	-0.0171	0.0094
19 C	-0.0005	-0.0039	0.0034	0.0003	-0.0074	0.0077
20 C	0.0014	0.0008	0.0006	0.0056	0.0001	0.0055
21 Br	-0.0147	-0.1215	0.1068	-0.0109	-0.1008	0.0899
22 Br	-0.0242	-0.1043	0.0801	-0.0183	-0.0837	0.0654
23 Br	-0.0061	-0.0611	0.0550	-0.0091	-0.0434	0.0343
24 Br	-0.0162	-0.0977	0.0815	-0.0119	-0.0775	0.0656
25 O	-0.0161	-0.0760	0.0599	-0.0172	-0.0900	0.0728
26 O	0.0132	-0.0572	0.0704	0.0099	-0.0694	0.0793
27 Na	-0.5207	-0.0876	-0.4331	-0.5237	-0.0806	-0.4431
28 C	-0.0051	0.0010	-0.0061	-0.0080	-0.0001	-0.0079
29 O	0.0030	-0.0035	0.0065	0.0016	-0.0061	0.0077
30 O	0.0058	-0.0223	0.0281	0.0035	-0.0242	0.0277
31 Na	-0.3660	-0.0525	-0.3135	-0.3687	-0.0480	-0.3207

CONCLUSION

The results and findings of this study revealed that wood saw dust from *Musanga cecropiode* is effective in the removal of EY due from aqueous solution. The removal efficiency of the wood saw dust depends on temperature, adsorbent dosage, concentration of the dye and period of contact. The adsorption behavior of the studied system conforms with some kinetic and isotherms models. The adsorption of the dye is spontaneous and exothermic. Quantum chemistry provides good information on the atoms/functional groups associated with the adsorption of the dye. Missing functional groups and the formation of new bonds also confirmed that the dye molecules are removed from the aqueous solution through adsorption.

ACKNOWLEDGEMENT

REFERENCES

1. EPA (2018) Drinking water standard and health advisory table. Office of water, US, Environmental Protection Agency, Washington.

2. Odoemelam SA, Eddy NO (2009) Studies on the use of oyster, snail and periwinkle shells as adsorbents for the removal of Pb2+. J Chem 6: 213-222.

3. Sciban M, Radetic B, Kevresan Z, Klasnja M (2007) Adsorption of heavy metals from electroplating wastewater by wood sadust. Resour Technol 98: 402-409.

4. Meena AK, Kadirvelu K, Mishra GK, Rajagopal C, Nagar PN (2008) Adsorptive removal of heavy metals from aqueous solution by treated sawdust Acacia Arabica. J Hazard Mater 150: 604-611.

5. Kant R (2012) Textile dyeing industry, an environmental hazard. Nat Sci 22: 26

6. Hassaan MA, ElNemr A (2017) Health and environmental impacts of dyes: Mini review. Am J Environ Sci Eng 13: 64-67.

7. Sdiri A, Higashi T (2012) Simultaneous removal of heavy metals from aqueous solution by natural limestones. Appl Water Sci 3: 29-39.

8. Adhnikan S, Manda S, Sarkar S, Kim D, Madras G (2017) Kinetics and mechanism of dye adsorption on WO3 nanoparticles. Appl Surf Sci 420: 472-482.

9. Odiongenyi AO (2019) Removal of ethyl violet dye from aqueous solution by graphite dust and nano graphene oxide synthesized from graphite dust. Commun Phys Sci 4: 103-109.

10. Odiongenyi AO, Afangide UN (2019) Adsorption and thermodynamic studies on the removal of congo red dye from aqueous solution by alumina and nano-alumina. Commu Phys Sci 4: 1-7.

11. Bharathi KS, Ramesh ST (2013) Removal of dyes using agricultural waste as low-cost adsorbent: A review. Appl Water Sci 34: 773-790.

12. Odoemelam SA, Emeh NU, Eddy NO (2018) Experimental and computational chemistry studies on the removal of methylene blue and malachite green dyes from aqueous solution by neem Azadiractha indica leaves. J Taibah Univ Sci 123: 255-265.

13. Badu M, Boatenf I, Boadi NO (2014) Evaluation of adsorption of textile dyes by wood sawdust. Res J Phy Appl Sci 31: 006-014.

14. Rahimi M (2007) Use of beech wood sawdust for adsorption of textile dyes. PJBS 102: 287-293.

15. Pinto T, Bezerra CWB, Silva DS, Filho ECD, Viera AP, et al. (2016) Sawdust derivatives for environmental application: Chemistry, functionalization and removal of textile dye from aqueous solution. An Acad Bras Cienc 883.

16. Eddy NO, Ekwumemgbo PA, Odoemelam SA (2008) Inhibition of the corrosion of mild steel in H2SO4 by 5-amino-1-cyclopropyl-7- [(3R, 5S) 3, 5-dimethylpiperazin-1-YL]-6, 8-difluoro-4-oxo-uinoline-3-carboxylic acid (ACPDQC). Int J Phys Sci 3: 1-6.

17. Eddy NO, Ameh P, Gimba CE, Ebenso EE (2011) GCMS studies on Anogessus leocarpus (AL) gum and their corrosion inhibition potential for mild steel in 0.1 M HCl. Int J Electrochem Sci 6: 5815-5829.

18. Eddy NO, Ameh P, Gimba EC, Ebenso EE (2012) Chemical information from GCMS of Ficus platyphylla gum and its corrosion inhibition potential for mild steel in 0.1 M HCl. Int J Electrochem Sci 7: 5677-569.

19. Okwunodulu FU, Eddy NO (2014) Equilibrium and thermodynamic consideration of Cd2+, Ni2+ and Pb2+ removal from aqueous solution onto treated and untreated Cola nitida waste biomass. Int J Sci Res 2: 567-569.

20. Nagy B, Manzatu C, Maicaneanu A, Indolean C, Lucian B, et al. (2017) Linear and nonlinear regression analysis for heavy metal removal using Agaricus bisporusmacrofungus. Arab J Chem 10: S3569-S3579.

21. Miyah Y, Labrichi A, Idrissi M, Boujraf S, Taouda H, et al. (2017) Assessment of adsorption kinetics for removal potential of crystal violet dye from aqueous solution using Moroccan pyrophyllite. J Assoc Arab Univ Basic Appl Sci 23: 20-28.

22. Nethaji S, Sivasamy A, Mandal AB (2013) Adsorption isotherms, kinetics and mechanism for the adsorption of cationic and anionic dyes onto carbonaceous particles prepared from Juglans regia shell biomass. Int J Environ Sci Tech 10: 231-242.

23. Padmavathy KS, Madhu G, Haseena PV (2016) A study on effects of pH, adsorbent dosage, time, initial concentration and adsorption isotherm study for the removal of hexavalaent chromium CRVI from wastewater by magnetite nanoparticle. International Conference on Emerging trends in Engineering Science ICETEST-2015 24: 585-594.

24. Elsagh A, Moradi O, Fakhri A, Najafi F, Alizadeh R, et al. (2017) Evaluation of the potential cationic dye removal using adsorption by grapheme and carbon nanotubes as adsorbents surfaces. Arab J Chem 10: S2862-S2869.

25. Bulut E, Ozacar M, Sengil IA (2008) Adsorption of malachite green onto nemtolite: Equilibrium and kinetic studies and process design. Micropor Mesopor Mat 115: 234-246.

26. Keskinkan O (2006) Isotherm models for predicting the dye adsorption potential of coon tail Ceratophyllum demersum and water milfoil Myriophyllum spicatum. Keskinkan/Adsorption Science and Technology 24: 321

27. Chiban M, Carja G, Lehutu G, Sinan F (2016) Equilibrium and thermodynamic studies for the removal of AsV ions from aqueous solution using dried plants as adsorbents. Arab J Chem 9: S988-S999.

28. Zhao D, Zhang W, Chen C, Wang X (2013) Adsorption of methyl orange dye onto multiwalled carbon nanotubes. Procedia Environ Sci 18: 890-895.

29. Santhi T, Manonmani S, Vasantha VS, Chang TT (2016) A new alternative adsorbent for the removal of cationic dyes from aqueous solution. Arab J Chem 9: S466-S474.

30. Tan KL, Hameed BH (2017) Insight into the adsorption kinetics model for the removal of contaminants from aqueous solutions. J Taiwan Inst Chem Eng 15: 1-24.

31. Weber WJ, Moris JC (1963) Kinetics of adsorption on carbon from solution. JSED 89: 31-59.

32. Eddy NO, Odiongenyi AO (2010) Corrosion inhibition and adsorption properties of ethanol extract ofHeinsiacrinataon mild steel in H2SO4. Pigm Resin Technol 385: 288-295.

33. Eddy NO, Essien NB (2017) Computational chemistry study of toxicity of some m-tolyl acetate derivatives insecticides and molecular design of structurally related products. In Silico Pharmacol 51: 14.

34. Eddy NO, Ita BI (2011) Experimental and theoretical studies on the inhibition potentials of some derivatives of cyclopenta-1, 3-diene. Int J Quantum Chem 11114: 3456-3473.

35. Eddy NO, Ita BI (2011) Theoretical and experimental studies on the inhibition potentials of aromatic oxaldehydes for the corrosion of mild steel in 0.1 M HCl. J Mol Model 17: 633-647.

36. Eddy NO, Awe FE (2018) Experimental and quantum chemical studies on ethanol extract of Phyllanthus amarus EEPA as a green corrosion inhibitor for aluminium in 1 M HCl. Port Electrochimica Acta 364: 231-247.

37. Eddy NO, Ameh PO, Essien NB (2018) Experimental and computational Chemistry studies on the inhibition of aluminum and mild steel in 0.1 M HCl by 3-nitrobenzoic acid. J Taibah Univ Sci 12: 545-556.

38. Eddy NO (2009) Modeling of the adsorption of Zn2+ from aqueous solution by modified and unmodified Cyperusesculentus shell. Elec J Env Agricult Food Chem 8: 1177-1185.

39. Eddy NO, Ita BI, Dodo SN, Paul ED (2002) Inhibitive and adsorption properties of ethanol extract of Hibiscus sabdariffa calyx for the corrosion of mild steel in 0.1 M HCl. Green Chem Lett Rev 5: 43-53.

40. Eddy NO, Ekwumemgbo PA, Odoemelam SA (2008) Inhibition of the corrosion of mild steel in H2SO4 by 5-amino-1-cyclopropyl-7-[(3R, 5S) 3, 5-dimethylpiperazin-1-YL]-6, 8-difluoro-4-oxo-uinoline-3-carboxylic acid (ACPDQC). Int J Phys Sci 3: 1-6.

41. Banerjee S, Chattopadhyaya MC (2017) Adsorption characteristics for the removal.

42. of a toxic dye, tartrazine from aqueous solutions by a low-cost agricultural by-product. Arab J Chem 10: S1629-S1628.

43. Bridgeman AJ, Cavglasso G, Ireland LR, Rothery J (2001) The Mayer bond order as a tool in inorganic Chemistry. J Chem Soc. Dalton Transaction 14: 2095-2108

44. Pathania D, Sharma S, Singh P (2017) Removal of methylene blue by adsorption onto activated carbon developed from Ficus caricabast . Arab J Chem 10: S1445-S1451.

45. Stevenson J, Sorenson B, Subtamaniam VH, Raiford J, Khlyabich PP, et al. (2017) Mayer bond order as a metric of complexation effectiveness in lead halide perovskite solutions. Chem Mater 29: 2435-2444.

46. Eddy NO, Momoh-Yahaya H, Oguzie EE (2015) Theoretical and experimental studies on the corrosion inhibition potentials of some purines for aluminum in 0.1 M HCl. J Adv Res 6: 203-216.

47. Ameh PO, Eddy NO (2018) Theoretical and Experimental Investigations of the Corrosion Inhibition Action of Piliostigma Thonningii Extract on Mild Steel in Acidic Medium. Commun Phys Sci 3: 27-42.

48. Amin MT, Alazba AA, Shafiq M (2015) Adsorptive removal of reactive black 5 from wastewater using bentonite clay: Isotherm, kinetics and thermodynamics. Sustainability 7: 15302-15318.